



Deposited via The University of Sheffield.

White Rose Research Online URL for this paper:

<https://eprints.whiterose.ac.uk/id/eprint/225874/>

Version: Published Version

---

**Article:**

Wannigama, D.L., Hurst, C., Monk, P.N. et al. (2025) tesG expression as a potential clinical biomarker for chronic *Pseudomonas aeruginosa* pulmonary biofilm infections. *BMC Medicine*, 23. 191. ISSN: 1741-7015

<https://doi.org/10.1186/s12916-025-04009-x>

---

**Reuse**

This article is distributed under the terms of the Creative Commons Attribution (CC BY) licence. This licence allows you to distribute, remix, tweak, and build upon the work, even commercially, as long as you credit the authors for the original work. More information and the full terms of the licence here:

<https://creativecommons.org/licenses/>

**Takedown**

If you consider content in White Rose Research Online to be in breach of UK law, please notify us by emailing [eprints@whiterose.ac.uk](mailto:eprints@whiterose.ac.uk) including the URL of the record and the reason for the withdrawal request.

RESEARCH

Open Access



# *tesG* expression as a potential clinical biomarker for chronic *Pseudomonas aeruginosa* pulmonary biofilm infections

Dharmika Leshan Wannigama<sup>1,2,3,4,5,6,7\*</sup>, Cameron Hurst<sup>8,9,10,11\*</sup>, Peter N. Monk<sup>12</sup>, Gunter Hartel<sup>9</sup>, William Graham Fox Ditcham<sup>4</sup>, Parichart Hongsing<sup>6,7†</sup>, Phatthranit Phattharapornjaroen<sup>13,14</sup>, Puey Ounjai<sup>15</sup>, Pattama Torvorapanit<sup>16</sup>, Kamonwan Jutivorakool<sup>16</sup>, Sirirat Luk-in<sup>17</sup>, Sumanee Nilgate<sup>2,3</sup>, Ubolrat Rirerm<sup>2,3</sup>, Chanikan Tanasatitchai<sup>2,3,6</sup>, Kazuhiko Miyanaga<sup>18</sup>, Longzhu Cui<sup>18</sup>, Naveen Kumar Devanga Ragupathi<sup>5,19,20</sup>, S. M. Ali Hosseini Rad<sup>21,22</sup>, Aisha Khatib<sup>23</sup>, Robin James Storer<sup>24</sup>, Hitoshi Ishikawa<sup>25</sup>, Mohan Amarasiri<sup>26</sup>, Somrat Charuluxananan<sup>27</sup>, Asada Leelahavanichkul<sup>2,28</sup>, Talerngsak Kanjanabuch<sup>29,30,31,32</sup>, Paul G. Higgins<sup>33,34†</sup>, Jane C. Davies<sup>35,36</sup>, Stephen M. Stick<sup>37,38,39†</sup>, Anthony Kicic<sup>37,38,39,40†</sup>, Tanittha Chatsuwana<sup>2,3\*</sup>, Kenji Shibuya<sup>41</sup> and Shuichi Abe<sup>1,6†</sup>

## Abstract

**Background** *Pseudomonas aeruginosa* infections in the lungs affect millions of children and adults worldwide. To our knowledge, no clinically validated prognostic biomarkers for chronic pulmonary *P. aeruginosa* infections exist. Therefore, this study aims to identify potential prognostic markers for chronic *P. aeruginosa* biofilm lung infections.

**Methods** Here, we screened the expression of 11 *P. aeruginosa* regulatory genes (*tesG*, *algD*, *lasR*, *lasA*, *lasB*, *pelB*, *phzF*, *rhlA*, *rsmY*, *rsmZ*, and *sagS*) to identify associations between clinical status and chronic biofilm infection.

**Results** RNA was extracted from 210 sputum samples from patients ( $n = 70$ ) with chronic *P. aeruginosa* lung infections (mean age; 29.3–56.2 years; 33 female). Strong biofilm formation was correlated with prolonged hospital stays (212.2 days vs. 44.4 days) and increased mortality (46.2% (18)). Strong biofilm formation is associated with increased *tesG* expression ( $P = 0.001$ ), influencing extended intensive care unit ( $P = 0.002$ ) or hospitalisation stays ( $P = 0.001$ ), pneumonia risk ( $P = 0.006$ ), and mortality ( $P = 0.001$ ). Notably, *tesG* expression is linked to the modulation of systemic and sputum inflammatory responses and predicts biofilm biomass.

**Conclusions** This study provides the first clinical dataset of *tesG* expression levels as a predictive biomarker for chronic *P. aeruginosa* pulmonary infections.

<sup>†</sup>Parichart Hongsing, Paul G. Higgins, Stephen M. Stick, Anthony Kicic and Shuichi Abe contributed equally to this work.

\*Correspondence:

Dharmika Leshan Wannigama

Dharmika.L@chula.ac.th

Cameron Hurst

cameron.hurst@cdu.edu.au

Tanittha Chatsuwana

tanittha.c@chula.ac.th

Full list of author information is available at the end of the article



**Keywords** TesG expression, Clinical biomarker, Chronic infections, *Pseudomonas aeruginosa*, Pulmonary biofilm, Respiratory infections, Chronic respiratory diseases

## Background

Lung diseases caused by *Pseudomonas aeruginosa* infections affect hundreds of millions of children and adults worldwide [1, 2]. *P. aeruginosa* is an opportunistic pathogen that can cause invasive and fulminant infections, including acute pneumonia in immunocompromised patients [1–4]. Remarkably, the same bacteria also cause chronic lung infections that can persist for months to years in individuals with cystic fibrosis (CF), chronic obstructive pulmonary disease (COPD), bronchiectasis, or lung cancer [1, 2, 4–6]. Chronic *P. aeruginosa* infections result from a dynamic and complex interplay between the pathogen and host via biofilm formation [1, 4]. Biofilms form where bacteria persist without causing overwhelming tissue injury, and the immune system fails to eradicate the pathogen [1]. Biofilm behaviours give *P. aeruginosa* a unique advantage in modulating host inflammation, dysregulating rapid pathogen clearance, and shifting between different infection phenotypes desensitised to antibiotic treatment [2, 4].

The pathogenic mechanisms of persistent pseudomonal respiratory diseases are far more complex than those of acute infections [1, 2, 4, 5]. Biofilm infections in the lungs often go beyond current laboratory-based diagnostic capabilities, making it difficult to make rational clinical decisions about treatment. The success of current antibiotic treatment is limited to most patients experiencing their first infection. However, recurrence is common with multi-drug resistance, and ultimately, progression to ineradicable chronic infection occurs in most adults. A primary characteristic of chronic bacterial biofilm lung infections is the lack of clear prognostic markers for diagnosing and managing the infections [1–5, 7, 8].

Several studies have distinguished between the molecular requirements for acute versus chronic infection [9–12]. Some of these requirements provide in-depth insights into the genes specifically needed for chronic *P. aeruginosa* infection [13]. One such gene that was significantly associated with chronic *P. aeruginosa* infection was *tesG*, the gene encoding TesG, a newly described type I secretion effector of *P. aeruginosa* that impairs alveolar lung macrophage function, promoting chronic infection and biofilm formation in the lung [9, 14]. Notably, *tesG* expression is controlled by the Rhl quorum-sensing (QS) system, and the protein is secreted into the extracellular environment by a genetically linked type I secretion system [9, 14].

*P. aeruginosa* is armed with its own specific QS system (PQS) and two common bacterial QS systems, LasI–LasR and RhlI–RhlR [5, 10]. QS systems play an important role in inducing biofilm formation and the establishing of chronic infection [5, 10]. In addition, bis-(3′–5′)-cyclic diguanosine monophosphate (c-di-GMP) and small RNAs (sRNAs) are also major players in chronic biofilm infections [1, 5, 10]. Additionally, contact-dependent growth inhibition (CDI) system in *P. aeruginosa* act as an interbacterial inhibition system and a bacterial virulence factor against a mammalian host (mouse) [15]. However, most related evidence is based on animal models [9]. Therefore, confirmation of the clinical relevance of these findings is important for a better understanding of the factors affecting biofilm-associated lung infections.

In 2019, the Antimicrobial Resistance and Stewardship Research Unit at the Faculty of Medicine, Chulalongkorn University, began deciphering the mechanism of chronic *P. aeruginosa* biofilm lung infections to identify potential prognostic markers in collaboration with King Chulalongkorn Memorial Hospital. Given that the newly described *tesG* gene is claimed to promote chronic lung infection, we profiled its association with clinical status and chronic biofilm infection in our retrospective cohort of patients, together with 10 other well-known regulatory genes (*algD*, *lasR*, *lasA*, *lasB*, *pelB*, *phzF*, *rhlA*, *rsmY*, *rsmZ*, and *sagS*). The genes *algD*, *lasR*, *lasA*, *lasB*, *pelB*, *phzF*, *rhlA*, *rsmY*, *rsmZ*, and *sagS* in *P. aeruginosa* play crucial roles in virulence, quorum sensing, and biofilm formation [16, 17]. *algD* is essential for alginate production, contributing to mucoid biofilms, while *pelB* aids in Pel polysaccharide biosynthesis [16, 17]. *lasR* regulates quorum sensing, controlling proteases like *lasA* (staphylolytic protease), and *lasB* (elastase), which degrade host tissues [16, 17]. *phzF* is involved in phenazine biosynthesis, enhancing oxidative stress resistance, while *rhlA* facilitates rhamnolipid production for biofilm disruption. *rsmY* and *rsmZ* are small RNAs that modulate virulence gene expression by sequestering RsmA [16, 17]. Lastly, *sagS* influences biofilm development and stress responses, playing a role in the switch between planktonic and sessile lifestyles [16, 17].

## Methods

### Study cohort, sample collection, and processing

We obtained, without any special selection, 240 sputum samples (collected as standard clinical routine work) from 81 patients who admitted to King Chulalongkorn

Memorial Hospital, Bangkok, Thailand, with culture-confirmed chronic *P. aeruginosa* respiratory infection. We excluded 30 of the 240 due to missing clinical data (11), culture contamination (9), or failed cultures (10), ultimately leaving 210 sputum samples from 70 patients for further analysis. All *P. aeruginosa* isolates were stored at the Department of Microbiology, King Chulalongkorn Memorial Hospital, Bangkok, Thailand, repository collection after standard characterisation and identification, including 16S rRNA sequencing as described previously [18]. The demographic characteristics of the patients, including age, sex, underlying disease or condition, length of hospital stay, susceptibility to antimicrobial agents, infection-related adverse events, pulmonary function measures, and discharge status/ mortality, were reviewed and obtained from medical records. Blood samples from patients were sent to a hospital laboratory for analysis, including differential cell count (DCC) and inflammatory marker data. The clinical strains, blood, and sputum used in this study had been isolated from patients as part of the standard patient care. Sputum samples were processed as described previously [12, 19] to stabilise RNA and preserve the original transcriptome of the bacteria. Sputum samples were added to 4 ml of freshly prepared sputum pre-lysis and preservation buffer (SLP buffer: 4 ml 1×DNA/RNA shield per 1–2 ml sputum sample, Zymo Research, USA; 200 mM Tris(2-carboxyethyl)phosphine, TCEP; 100 µg ml<sup>-1</sup> Proteinase K) and vigorously shaken by hand until the samples were homogenous and completely lysed. Stabilised samples were initially processed on ice and stored at –80°C until needed.

#### RNA extraction

Total RNA was extracted and assayed from sputum samples as described previously [12, 19]. Briefly, pre-lysed samples stored in SLP buffer (SLP buffer: 4 ml 1×DNA/RNA shield per 1–2 ml sputum sample, Zymo Research, USA; 200 mM Tris(2-carboxyethyl)phosphine, TCEP; 100 µg ml<sup>-1</sup> Proteinase K) were transferred to a 15-mL centrifuge tube prefilled with 1 volume of TRIzol LS Reagent (Invitrogen) and 1 mL of zirconium/glass beads (0.1 mm diameter, Carl Roth) and were bead-beaten on a horizontal shaker (BIOSPEC 2500 RPM) four times for 1 min, to ensure complete lysis of human and bacterial cells. After each iteration, the sample temperature was lowered by incubating the tube on ice for 1 min. Samples in TRIzol LS were then briefly centrifuged to pellet the beads, the supernatant was split into multiple 1-mL aliquots, and 270 µL of chloroform was added. After shaking vigorously for 15 s, the samples were incubated for 2 min at room temperature and then centrifuged at 13,000×g at 4°C for 30 min to separate the aqueous phase. All RNA species longer than 17 nt were purified

from the recovered aqueous phase using a RNA Clean & Concentrator-25 (RCC) kit (Zymo Research), according to the manufacturer's protocol. After initial quality control and quantification on a Nanodrop (280/260 and 280/230 ratios were always higher than 1.7 and 2.2, respectively), 50–100 µg of total RNA was treated with 6–10 U of Turbo DNase (Invitrogen) (10X TURBO DNase Buffer (5 µL) and 6–10 U of TURBO DNase (2 µL), adjusting the final volume 50 µL with nuclease-free water; the mixture was incubated at 37°C for 30 min), and the products were purified on columns using the RCC kit. Because RNA extracted from sputum samples results in partially degraded samples, to increase RNA quality and remove intrinsic background noise, we selected the RNA, recovering RNA species longer than 200 nt following the protocol supplied with the on-column purification kit. The recovered RNA was quantified using fluorometric quantitation using a Qubit RNA BR Assay kit (Invitrogen), and the fragmentation state and RNA quality were assayed using an RNA Nano kit on an Agilent Bioanalyzer 2100 machine (Agilent Technologies). When needed, DNAase-treated samples were concentrated through ethanol precipitation (Additional file 1). First-strand cDNA (From each sample, 0.5 µg of total RNA was used) synthesis was performed using SuperScript II Reverse Transcriptase (Invitrogen) according to the manufacturer's instructions in an RNase-free environment using RNase-free consumables and RNase-free reagents (Additional file 1). cDNA was stored at –20°C until use.

#### Quantitative PCR

To determine the expression of *algD*, *lasR*, *lasA*, *lasB*, *pelB*, *phzF*, *rhlA*, *rsmY*, *rsmZ*, *sagS*, and *tesG* (Additional file 1 Table S1) [9, 12, 20–22], quantitative PCR was performed using an iTaq Universal SYBR Green One-Step Kit (Bio-Rad) and a CFX Connect Real-Time PCR Detection System (Bio-Rad) according to the manufacturer's instructions. Reverse-transcribed total RNA from the sputum of patients chronically infected with *P. aeruginosa* was used as the template. Gene expression was calculated by the  $2^{-\Delta\Delta CT}$  method using *hptB* (Histidine-containing phosphotransfer protein-B (HptB) is one of the key regulatory gene in *Pseudomonas aeruginosa*) as a reference [12, 23]. All the experiments were independently repeated three times.

#### Bacterial strains and growth conditions

The biofilm-positive reference strain *P. aeruginosa* PAO1 (ATCC 15692), and clinical isolates were cultured on Müller–Hinton agar (Sigma-Aldrich) plates at 37°C (Additional file 1). The strains were stored at –80°C in tryptic soy broth (Sigma-Aldrich) supplemented with

15% glycerol until they were used in subsequent experiments, for which they were suitably anonymised.

#### Antibiotics and chemotherapy reagents

Amikacin, ciprofloxacin, colistin, ceftazidime, piperacillin/tazobactam, levofloxacin, and doripenem were obtained from Sigma-Aldrich. Susceptibility to fosfomycin (Wako Chemicals) was determined by supplementation with 25 µg/mL glucose-6-phosphate (Sigma-Aldrich). The concentrations of all the antimicrobial agents were adjusted to the susceptibility breakpoint concentrations recommended by the Clinical and Laboratory Standards Institute (CLSI)<sup>24</sup> and the European Committee on Antimicrobial Susceptibility Testing (EUCAST) [24].

#### Minimal inhibitory concentrations for planktonic cells

MICs were established using the standard broth microdilution method according to the criteria in the EUCAST [24] (criteria for *Enterobacteriaceae* for fosfomycin only and CLSI guidelines) [25] (Additional file 1). *E. coli* ATCC 25922 and *P. aeruginosa* ATCC 27853 were used as quality control strains.

#### Sputum biofilm visualisation using PNA FISH

Sputum smears were analysed using fluorescence in situ hybridisation (FISH) using peptide nucleic acid (PNA) probes (5'-GCTGAACCACTACG-3', 5'-CCCGCCCGTATC AAA-3', 5'-CTGAATCCAGGAGCA-3', and 5'-AACTTGCTGAACCAC-3'). Probe sequences were synthesized by Panagene (Daejeon, South Korea), and each oligonucleotide N-terminus was attached to a fluorochrome (Texas Red and FITC), via a double 8-amino-3, 6-dioxaoctanoic acid linker [26, 27]. The stock solution (at 100 mM) of each PNA probe was obtained by solubilising the powder in 10% (vol/vol) of acetonitrile and 1% (vol/vol) of trifluoroacetic acid. A mixture of PNA probes in hybridisation solution (10% (wt/vol) dextran sulphate, 10 mM NaCl, 30% (vol/vol) formamide, 0.1% (wt/vol) sodium pyrophosphate, 0.2% (wt/vol) polyvinylpyrrolidone, 0.2% (wt/vol) Ficoll (Type 400), 5 mM disodium EDTA, 0.1% (vol/vol) Triton X-100, and 50 mM Tris-HCl) was added to each section, and the mixture was hybridised on a PNA FISH workstation at 55°C for 90 min covered by a lid as described previously [26, 27]. The slides were washed for 30 min at 55°C in wash solution (AdvanDx) and the probes quantified using a confocal laser scanning microscopy. Biofilm structure was visualised by staining with Wheat Germ Agglutinin (WGA) conjugates Alexa Fluor 488 dye; (The original Alexa Fluor 488 dye, which is bright green, was pseudo-coloured magenta during confocal analysis using the pseudo-colour feature in confocal software to distinguish the image

from bacterial cell pictures), as described previously [28]. Briefly, a staining solution of WGA-Alexa Fluor 488 was prepared at a final concentration of 5 µg/ml in PBS and 50 µl added to the sputum smears. The samples were then incubated in the dark at room temperature for 30 min to allow specific binding to N-acetylglucosamine residues in the biofilm matrix. Following incubation, excess dye was removed by gently washing the sputum smears one time with PBS (100 µl).

#### Biofilm formation *in vitro*

Biofilm formation in a 96-well-microtitre-plate format was performed as described previously [18, 29]. Initially, a pure culture of a single colony of *P. aeruginosa* was inoculated into 2 mL of MHIIB medium in a tube and incubated in an orbital shaker (200 rpm) at 37°C overnight for approximately 16 h. Subsequently, a subculture was prepared from the overnight culture by diluting it with fresh MHIIB medium (Additional file 1) [18, 29–45] to an optical density (OD) of 0.02 at 600 nm ( $5 \times 10^7$  CFU/mL) and 100 µL aliquots were added in triplicate to flat-bottomed 96-well polystyrene microtitre plates (SPL Life Sciences), with uninoculated MHIIB medium (100 µL) in triplicate as a negative control. The plates were incubated at 37°C for 24 h.

#### Biofilm quantification and classification for assays *in vitro*

Two methods were used to quantify and classify the biofilm by Crystal Violet staining (0.1%) with modifications and confocal laser scanning microscopy using live/dead bacteria staining for confirmation [18, 29]. For Crystal Violet staining, the mean absorbance (OD at 550 nm) and standard deviation (SD) were calculated for all the strains and negative controls tested. Quantification was performed in triplicate and repeated independently three times [18, 29]. The cut-off value ( $OD_{\beta}$ ) was defined as 3SD above the mean OD of the negative controls:  $OD_{\beta} = \text{average OD of the negative controls} + 3SD$  of negative controls, and was calculated separately for each microtitre plate. The OD of a tested strain was expressed as the mean OD of the strain minus the  $OD_{\beta}$  ( $OD = \text{mean OD of a strain} - OD_{\beta}$ ). The clinical isolates were classified as described previously ( $OD \leq OD_{\beta} =$  no biofilm producer;  $OD_{\beta} < OD \leq 2 \times OD_{\beta} =$  weak biofilm producer;  $2 \times OD_{\beta} < OD \leq 4 \times OD_{\beta} =$  moderate biofilm producer;  $4 \times OD_{\beta} < OD =$  strong biofilm producer) [18, 29]. Confocal laser scanning microscopy (CLSM) with live/dead bacterial staining in 96-well microtiter plates was performed, and biofilm quantification was analysed using the MATLAB-based tool PHLIP, following the previously described method [46]. For CLSM analysis, supernatants are carefully removed and biofilms are subsequently stained with the LIVE/DEAD Bacterial Viability Kit

(Invitrogen) according to the manufacturer's protocol (Syto9 and PI are diluted in the ratio of 1:300 in 100  $\mu\text{L}$  of sodium chloride solution containing 5% (vol/vol) DMSO (100%); final concentration of 1.4  $\mu\text{M}$  of SYTO9 and 8.3  $\mu\text{M}$  of PI (propidium iodide) and incubate at room temperature in the dark for 15 min). MATLAB-based tool PHLIP (without connected volume filtration) were used to calculate descriptive parameters of biofilms (including biovolume, substratum coverage, area-to-volume ratio, spatial spreading and 3D colocalization) from the integrated total of each individual slice of a thresholded  $z$ -stack as described previously [28, 34–36, 38, 40, 42, 46–48]. The calculation of the different proportions of green (live bacteria) as well as red and yellow/colocalised (dead bacteria) biovolumes from the analysed stacks were using the “colocalization in 3D” value and the parameters “red,” “green,” and “total biovolume” (in  $\mu\text{m}^3$ ) generated by the PHLIP software as described previously [46].

#### Alginate measurement assay

To measure the amount of alginate produced by the *P. aeruginosa* clinical isolates, the samples were assayed as previously described [49]. Briefly, the isolates were grown in 5 mL of LB broth with orbital shaking at 200 rpm at 37°C until the cultures reached an  $\text{OD}_{600}$  of 2.0. Bacterial cells were then collected by centrifugation at  $7000\times g$  for 20 min and suspended in 1 mL of PBS buffer. Simultaneously, another culture was used to correlate the  $\text{OD}_{600}$  2.0 with the dry cell weight. To remove any contaminants, such as RNA and DNA from the alginate, the samples were treated with RNase A (Promega) (4 mg/ml) and DNase I (Sigma) (10 mg/mL) and incubated at 37°C for 1 h. To remove the cells, the mixture was vortexed and centrifuged at  $8000\times g$  for 20 min. The remaining alginate in the supernatant was then precipitated with 25 mL of 95% ethanol and collected by centrifugation at  $10,000\times g$  for 30 min and suspended in 2 mL of 0.85% NaCl. The uronic acid concentration was determined by a standard colorimetric assay (m-hydroxydiphenyl method; Additional file 1).

#### Quantification of pyocyanin generated in biofilms

The amount of pyocyanin produced by *P. aeruginosa* clinical isolate biofilms was quantitatively measured as described previously with modifications [50, 51]. Briefly, the isolates were grown in 5 mL of LB broth culture at 37°C with shaking (200 rpm) for 16 h and centrifuged ( $7000\times g$  for 20 min). The resultant supernatant was subsequently used to quantify pyocyanin. In brief, 600  $\mu\text{L}$  of chloroform was added to 1 mL of supernatant, and the tube was vortexed twice for 10 s. The tubes were then centrifuged at 10,000 rpm for 10 min, after which the lower organic phase was transferred to a new tube

containing 300  $\mu\text{L}$  of 0.2 N HCl. The tubes were vortexed twice for 10 s each time and centrifuged at 10,000 rpm for 2 min. The  $\text{OD}_{520}$  of the upper phase was measured and multiplied by 17.072 to calculate the concentration of pyocyanin in mg/mL.

#### Measurements of extracellular DNA (eDNA) in biofilms

The eDNA concentration in *P. aeruginosa* biofilms was determined by PicoGreen fluorescence staining (Quant-iT Invitrogen) in a 96-well microtitre plate biofilm as described previously with modifications [52]. Briefly, freshly prepared PicoGreen dye solution diluted in TE buffer (1  $\mu\text{L}$  PicoGreen<sup>®</sup> dye diluted in 199  $\mu\text{L}$  TE buffer) was added to each well at a ratio of 1:1, and the eDNA concentration was measured on a microplate-reading fluorescence spectrophotometer (Varioskan Flash Multimode Reader; Thermo Fisher Scientific) at 470 nm excitation and 525 nm detection. To verify reproducibility, eDNA production in the biofilm cultures was also quantified using laser scanning fluorescence microscopy (Zeiss Axiovert 200 M) after staining with propidium iodide (30  $\mu\text{M}$ ) (BacLight Live/dead staining kit) [46].

#### Quantification of c-di-GMP

To measure the amount of c-di-GMP produced by *P. aeruginosa*, clinical isolates were assayed by liquid chromatography–mass spectrometry (LCMS) (Thermo Fisher Scientific) as previously described [53]. A 15 mL of *P. aeruginosa* cell culture was harvested and washed twice with 1 mM ammonium acetate. An aliquot of cells was used for protein quantification, and the remaining cells were washed twice with 1 mM ammonium acetate and lysed in 1 mL of acetonitrile/methanol/ddH<sub>2</sub>O (40:40:20) using a probe tip ultrasonicator (30% amplitude, 5 s on/off cycles for 1 min on ice). Cell debris was removed by centrifugation at  $13,000g$  at 4°C for 3 min. The supernatant containing nucleotides was lyophilised using a vacuum concentrator and resuspended in 100  $\mu\text{L}$  of 1 mM ammonium acetate. c-di-GMP concentrations were determined by comparing to a standard reference. Chromatographic separation was achieved using a Nucleodur C18 Pyramid column (2 $\times$ 50 mm, 3  $\mu\text{m}$ ) at 40°C, with a flow rate of 0.3 mL/min and a 10  $\mu\text{L}$  injection volume. A gradient of ammonium acetate buffer (1 mM ammonium acetate buffer containing 0.1% acetic acid) and acetonitrile (acetonitrile with 0.1% (v/v) acetic acid) were used. Solvent gradient conditions were as follows: 0% B from 0 to 3 min; 10% B at 3 min; 90% from 4 to 5th min; 0% B at 5.5th min and equilibrated for 4.5 min. The total run time was 10 min.

Detection was conducted in positive ion electrospray ionisation (ESI+) mode. The heater and capillary temperatures were set to 300°C. Sheath, auxiliary, and sweeper

gas flows were 40, 15, and 1 arb. units, respectively. The source voltage was 3.5 kV. For quantitation, the scan type in selected ion monitoring mode was utilised at high resolution (60,000), with an AGC target of  $1 \times 10^6$ . Quantification was achieved through an MS/MS experiment using collision-induced dissociation (CID) with normalised collision energy set to 20% of maximum, with an isolation width of 1 Da and an activation time of 30 ms.

To quantify the proteins, the cells were treated with 1 mL of 5 M NaOH at 95°C for 5 min. After the samples were cooled for 15 min, the proteins were processed using a Qubit protein assay kit (NanoOrange dye) and quantified using a Qubit 2.0 fluorometer (Invitrogen). The concentration of c-di-GMP was then normalised to the protein concentration.

### Cytotoxicity and proteolytic assessment

To determine the cytotoxicity of *P. aeruginosa*, clinical isolates, A549 cells were seeded ( $1.0 \times 10^4$  cells/well) in 96-well tissue culture plates containing 100  $\mu$ l of Dulbecco's modified Eagle's medium (DMEM) and allowed to grow at 37°C for 16 to 18 h to obtain 80 to 90% monolayer confluency. Culture supernatants were removed, the monolayer was washed once with PBS buffer (100  $\mu$ l). For inoculation, the fresh *P. aeruginosa* biofilm mixture (biofilm formation described under the “[Biofilm formation in vitro](#)” section and mixture was prepared by harvesting biofilms from 96-well plate wells using mini cell scrapers) containing bacteria cells and biofilm matrix substance were resuspended and diluted in DMEM or LB medium or culture supernatants as indicated to a concentration about  $1 \times 10^7$  CFU per ml or otherwise indicated. Thereafter, 100  $\mu$ l of the biofilm dilution was applied to the A549 cell monolayers at a multiplicity of infection (MOI) of 50. After infection for 4 h at 37°C, A549 cell viability was measured by WST-1 assay, which quantifies mitochondrial metabolic activity, following the manufacturer's instructions (Roche).

Proteolytic activity was measured by azocasein assay. The azocasein assay was performed using an adapted method based on earlier studies, with some modifications [54]. A 3% w/v azocasein solution in 50 mM 3-Morpholinopropanesulfonic Acid (MOPS), 1 mM CaCl<sub>2</sub>, pH 6.7, was prepared. Two aliquots of 100  $\mu$ l of *P. aeruginosa* biofilm mixture containing bacteria cells and biofilm matrix substance were mixed with 100  $\mu$ l 3% w/v azocasein and 300  $\mu$ l 50 mM Na<sub>2</sub>HPO<sub>4</sub>, and incubated for 1 h at 37°C. The reaction was stopped by adding 500  $\mu$ l 20% trichloroacetic acid (TCA). Samples were centrifuged (10 min, 25°C, 12,000  $\times g$ ) and 150  $\mu$ l of the supernatant were transferred to triplicate wells in 96-well microtiter plates, which contained 50  $\mu$ l 1 M NaOH. Absorbance was measured with a spectrophotometer

(Multi-Mode Microplate Reader, Synergy™ 2, BioTeK) at 366 (used as reference to check for background absorbance or interference) and 450 nm (as it corresponds to the absorbance of the released azo-dye fragments, which indicate protein hydrolysis). Proteolytic activity was calculated by subtracting the absorbance of the non-incubated sample from the value for the incubated sample and expressed as  $\Delta A \times h^{-1} \times mL^{-1}$ .

### Data/statistical analysis

Patient characteristics were summarised using means and standard deviations for continuous variables, and counts and percentages for categorical variables. Preliminary investigations of the associations between patient variables and biofilm formation category (moderate or strong) were assessed using independent sample *t* tests for continuous outcomes, log-rank tests for time-to-event variables, and chi-square tests of independence for categorical variables. Within-gene expression correlations and gene expression–inflammatory marker intercorrelations were evaluated using Pearson correlation coefficients with correlograms used to display the strength and direction of the correlations. Formal multivariable modelling of the time-to-event outcomes (mortality, length of hospital stay, and length of ICU stay) was conducted using Cox proportional hazard regression analysis, and multivariable modelling of binary outcomes was conducted using binary logistic regression analysis. The diagnostic utility of gene expression in predicting the biofilm formation category was initially assessed using sensitivity, specificity, and diagnostic accuracy (along with their 95% CIs). The diagnostic accuracy of the expression of the three genes *tesG*, *lasR*, and *pelB* was further investigated using receiver operating characteristic curves. All analyses were conducted using the R statistical package [55], and a significance level of 0.05 was used for all tests of statistical inference.

## Results

### Patient characteristics

The patient population consisted of 70 individuals with varying degrees of biofilm formation, with 31 individuals classified as having moderate biofilm formation and 39 individuals classified as having strong biofilm formation (Table 1). The population included male and female patients, with slightly more female patients in the moderate biofilm formation group. The age of the patients ranged from 1 month to 91 years, with a mean age of 56.3 years in the moderate biofilm formation group and 40.9 years in the strong biofilm formation group. Patients in the population had various diagnoses at hospital admission, including cancer, cerebrovascular disease, chronic respiratory disease, and congestive

**Table 1** Clinical characteristics of patients with chronic *P. aeruginosa* lung infection

	Biofilm formation category		P
	Moderate (n = 31)	Strong (n = 39)	
Sex			
Female (%)	12 (38.7)	10 (25.6)	0.36
Age (mean (SD))	56.3 (29.4)	40.9 (30.2)	0.036
Diagnosis on hospital admission (%)			0.56
Cancer	8 (25.8)	5 (12.8)	
Cerebrovascular disease	4 (12.9)	8 (20.5)	
Chronic cognitive deficit	1 (3.2)	4 (10.3)	
Chronic respiratory disease	3 (9.7)	6 (15.4)	
Congestive heart failure	5 (16.1)	5 (12.8)	
Connective tissue disease	3 (9.7)	1 (2.6)	
Diabetes mellitus	2 (6.5)	1 (2.6)	
Myocardial infarction	1 (3.2)	1 (2.6)	
Peripheral vascular disease	4 (12.9)	6 (15.4)	
Renal disease	0 (0.0)	2 (5.1)	
Length of hospital stay (LOSH) (Median)	44.3 (IQR=22.3)	212.2 (IQR= 123.8)	0.0010
Length of stay intensive care unit (LOSICU) (Median)	12.6 (IQR=17.7)	38.4 (IQR=42.3)	0.0020
Co-infection (%)			0.55
No co-infection	20 (64.5)	30 (76.9)	
<i>Staphylococcus aureus</i>	1 (3.2)	1 (2.6)	
<i>Klebsiella pneumoniae</i>	4 (12.9)	2 (5.1)	
<i>Stenotrophomonas maltophilia</i>	1 (3.2)	1 (2.6)	
<i>Acinetobacter baumannii</i>	1 (3.2)	3 (7.7)	
<i>Enterobacter spp.</i>	2 (6.5)	0 (0.0)	
Herpes simplex virus (HSV)	1 (3.2)	1 (2.6)	
<i>Haemophilus influenzae</i>	0 (0.0)	1 (2.6)	
Cytomegalovirus (CMV)	1 (3.2)	0 (0.0)	
Adverse events (%)			0.89
No adverse events	12 (38.7)	14 (35.9)	
Cardiac	1 (3.2)	2 (5.1)	
Gastrointestinal	16 (51.6)	17 (43.6)	
Hematologic	0 (0.0)	1 (2.6)	
Hepatobiliary	1 (3.2)	2 (5.1)	
Neurologic	0 (0.0)	1 (2.6)	
Renal	1 (3.2)	2 (5.1)	
Mortality (%)	0 (0.0)	18 (46.2)	0.0010
Multi-drug resistance	10 (32.3)	19 (48.7)	0.25
Pneumonia (%)			0.0060
Community-acquired pneumonia (CAP)	23 (74.2)	14 (35.9)	
Hospital-acquired pneumonia (HAP)	2 (6.5)	7 (17.9)	
Ventilator-associated pneumonia (VAP)	6 (19.4)	18 (46.2)	

heart failure (Table 1). Confocal imaging of sputum samples from patients with chronic *P. aeruginosa* infection revealed distinguishable characteristics between patients with moderate to ( $1.78 \times 10^6 \mu\text{m}^3 \mu\text{m}^{-2}$ ) and strong biofilms ( $3.27 \times 10^6 \mu\text{m}^3 \mu\text{m}^{-2}$ ) (Fig. 1a–d). In the strong biofilm (Fig. 1a and b), the bacterial cells are

densely packed, as indicated by the intense green/yellow staining, and the biofilm matrix appears robust, a tightly formed extracellular polymeric substance (EPS) matrix, and well-structured, shown by the prominent pseudo coloured magenta staining. In contrast, the

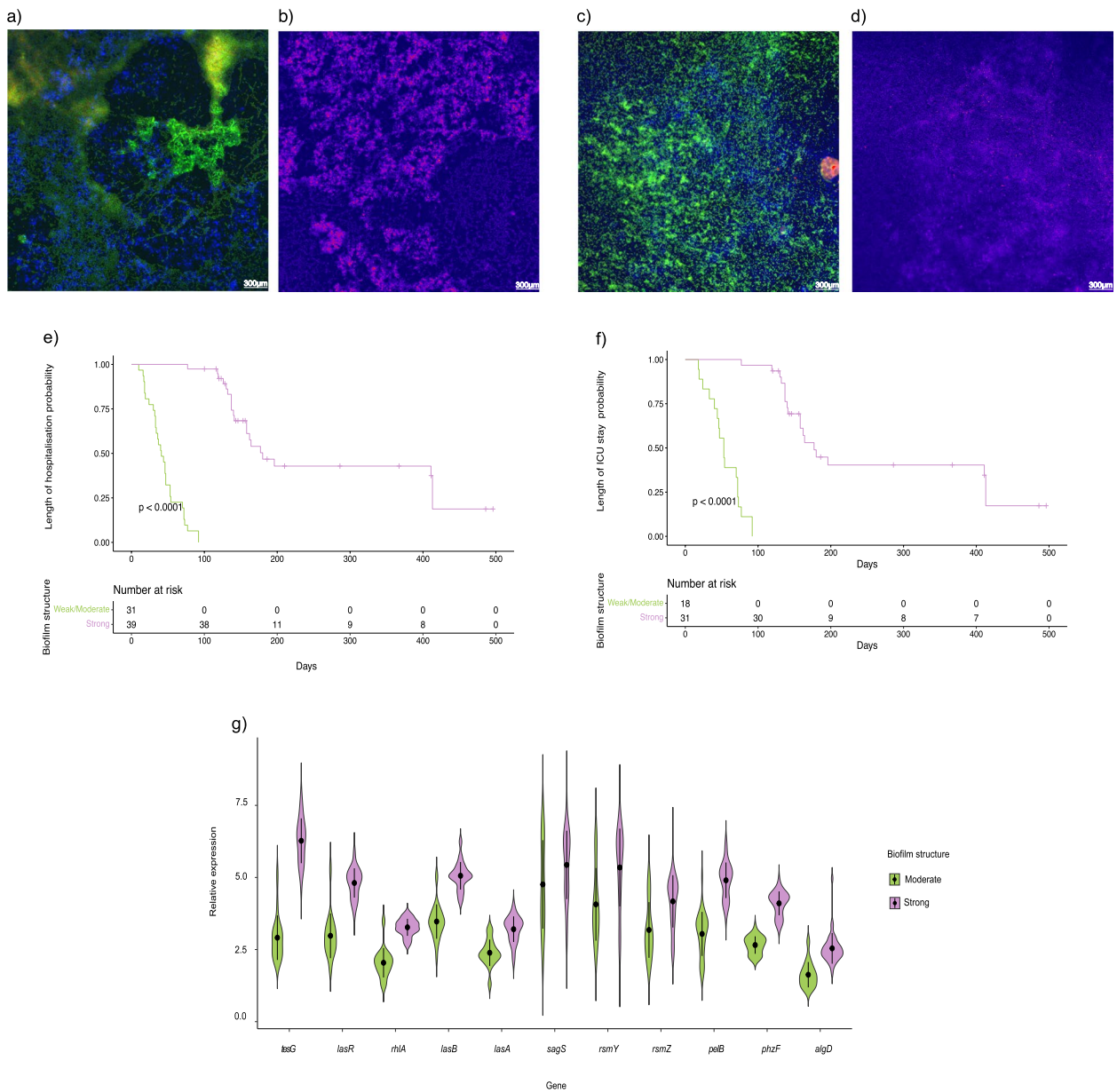


**Fig. 1** Confocal imaging of sputum from a patient with chronic *P. aeruginosa* infection **a** bacteria cells from strong biofilm (bacteria cells staining by PNA FISH probes; green/yellow, Hoechst blue for DNA), **b** strong biofilm structure only (staining with Wheat Germ Agglutinin (WGA) conjugates Alexa Fluor 488 dye; (pseudo coloured magenta), Hoechst blue for DNA), **c** bacteria cells from moderate biofilm (bacteria cells staining by PNA FISH probes; green/yellow, Hoechst blue for DNA), and **d** moderate biofilm structure only (Wheat Germ Agglutinin (WGA) conjugates Alexa Fluor 488 dye (pseudo coloured magenta), Hoechst blue for DNA). Sputum samples for images were obtained from two different patients. Survival analysis of biofilm structure (biomass) in terms of **e** length of hospitalisation and **f** length of ICU stay among patients with chronic *P. aeruginosa* lung infection ( $n = 70$ ). **g** Bacterial sputum gene expression level in relation to biofilm biomass among patients with chronic *P. aeruginosa* lung infection ( $n = 70$ )

moderate biofilm (Fig. 1c and d) shows reduced bacterial density, with less intense green/yellow staining and a weaker, less cohesive biofilm structure, as evidenced by lighter pseudo coloured magenta staining.

**Strong biofilm formation is linked to longer hospital stays, higher mortality, and increased risk of pneumonia**  
 The median length of hospital stay was 44.4 days (IQR=22.3) in the moderate biofilm formation group and 212.2 days in the strong biofilm formation group.

The median length of stay in the intensive care unit was 12.6 days in the moderate biofilm formation group and 38.4 days in the strong biofilm formation group (Table 1). Patients with strong biofilm formation had a longer hospital stays and longer stays in the intensive care unit than did those with moderate biofilm formation (Table 1) (Fig. 1e and f). Mortality was observed only in the strong biofilm formation group, at a rate of 46.2% (18/70). Patients with strong biofilm formation had a significantly ( $P=0.001$ ) greater mortality rate than did those with moderate biofilm formation (Table 1).

The incidence of pneumonia also varied significantly between the two groups, with a higher percentage of patients with strong biofilm formation having hospital-acquired pneumonia (HAP) and ventilator-associated pneumonia (VAP) (Table 1).

Furthermore, the incidence of co-infection did not differ significantly between the moderate and strong biofilm formation categories (Table 1). However, patients with strong biofilm formation had a 3 incidence of *Acinetobacter baumannii* co-infection than did those with moderate biofilm formation [1] incidence. There were no significant differences in the number of diagnoses at hospital admission between the two groups except for chronic cognitive deficit and chronic respiratory disease. More patients with chronic cognitive deficits were in the strong biofilm formation group, while more patients with chronic respiratory disease were in the moderate biofilm formation group (Table 1).

The adverse events were similar in both groups, with most patients experiencing gastrointestinal adverse events (Table 1). Multi-drug resistance did not differ

significantly between the two groups. Moreover, there was no significant difference between the sexes in terms of biofilm formation.

#### The expression of *tesG* is associated with prolonged ICU stay and hospitalisation

The gene expression levels of *tesG*, *lasR*, *rhIA*, *lasB*, *lasA*, *sagS*, *pelB*, and *algD* were significantly associated with longer hospitalisation (LOHS) or ICU (LOICU) stays (Table 2). However, *rsmY* and *rsmZ* were found to be associated only with longer LOHS. Notably, the expression of *tesG*, *lasR*, *rsmY*, *rsmZ*, *pelB*, *phzF*, and *algD* was associated with mortality, although no significant difference was observed (Table 2). By contrast, *sagS* was associated with a significantly lower risk of mortality (HR=0.182, 95% CI 0.075, 0.441).

#### Gene expression is associated with producing a strong biofilm structure and the risk of having pneumonia with adverse events

The gene expression of *tesG*, *lasR*, *rhIA*, *lasB*, *lasA*, *rsmY*, *rsmZ*, *pelB*, and *algD* differed significantly (all  $P=0.001$ ) between moderate and strong biofilms, as shown in Fig. 1g. Furthermore, the expression levels of these genes were positively correlated with the development of a strong biofilm structure, as indicated in Table 3.

All the tested genes were significantly associated with the development of pneumonia including CAP/HAP or VAP (Table 3). However, *tesG*, *lasR*, *rhIA*, *lasB*, *sagS*, *rsmY*, *rsmZ*, *pelB*, *phzF*, and *algD* were significantly associated only with worsening pneumonia status within 7 days. No significant relationships were detected between

**Table 2** Relationships between gene expression and length of hospital stay (LOHS), length of ICU stay (LOICU) and mortality in patients with chronic *P. aeruginosa* lung infection ( $n=70$ ) based on the hazard ratio (HR) as standardised (Z score) adjusted for sex and age.  $P < 0.05$  was considered to indicate significance

	Length of hospital stay (LOHS)	Length of ICU stay (LOICU)	Mortality
	HR (95% CI) <i>P</i>	HR (95% CI) <i>P</i>	HR (95% CI) <i>P</i>
Gene expression			
<i>tesG</i>	0.13 (0.07, 0.23) 0.0010	0.15 (0.074, 0.29) 0.0010	1.29 (0.21, 7.92) 0.786
<i>lasR</i>	0.36 (0.26, 0.51) 0.0010	0.44 (0.29, 0.67) 0.0010	1.11 (0.27, 4.49) 0.884
<i>rhIA</i>	0.35 (0.25, 0.49) 0.0010	0.43 (0.29, 0.65) 0.0010	0.96 (0.25, 3.67) 0.955
<i>lasB</i>	0.32 (0.23, 0.46) 0.0010	0.34 (0.21, 0.55) 0.0010	0.79 (0.27, 2.39) 0.685
<i>lasA</i>	0.5 (0.38, 0.66) 0.0010	0.54 (0.37, 0.79) 0.0010	0.94 (0.48, 1.83) 0.850
<i>sagS</i>	0.49 (0.35, 0.69) 0.0010	0.54 (0.33, 0.88) 0.013	0.18 (0.06, 0.44) 0.0010
<i>rsmY</i>	0.66 (0.50, 0.86) 0.002	0.81 (0.58, 1.14) 0.224	1.54 (0.84, 2.82) 0.165
<i>rsmZ</i>	0.59 (0.44, 0.79) 0.0010	0.77 (0.53, 1.09) 0.145	1.42 (0.79, 2.56) 0.238
<i>pelB</i>	0.29 (0.19, 0.43) 0.0010	0.27 (0.16, 0.45) 0.0010	0.82 (0.25, 2.70) 0.745
<i>phzF</i>	0.23 (0.15, 0.36) 0.0010	0.28 (0.16, 0.47) 0.0010	1.61 (0.45, 5.8) 0.462
<i>algD</i>	0.31 (0.21, 0.47) 0.0010	0.34 (0.21, 0.56) 0.0010	1.11 (0.63, 1.969) 0.701

HR Hazard ratio, CI Confidence intervals

**Table 3** Relationships between gene expression and biofilm structure, HAP, VAP or CAP infection; and pneumonia status within 7 days in the patients with chronic *P. aeruginosa* lung infection ( $n=70$ ) based on the odds ratio (OR) as standardised (Z score) adjusted for sex and age:  $P<0.05$  was considered to indicate significance

	Biofilm structure	HAP, VAP or CAP	Pneumonia status within 7 days
	OR (95% CI) <i>P</i>	OR (95% CI) <i>P</i>	OR (95% CI) <i>P</i>
Gene expression			
<i>tesG</i>	3115.14 (2.31, 4203918.49) 0.025	2.48 (1.44, 4.26) 0.001	0.49 (0.29, 0.85) 0.01
<i>lasR</i>	36.87 (6.85, 198.42) 0.0010	2.29 (1.36, 3.89) 0.002	0.45 (0.26, 0.79) 0.004
<i>rhIA</i>	46.32 (7.42, 289.16) 0.0010	1.91 (1.14, 3.19) 0.014	0.58 (0.34, 0.97) 0.036
<i>lasB</i>	141.22 (8.23, 2424.23) 0.0010	2.14 (1.24, 3.68) 0.006	0.53 (0.30, 0.92) 0.021
<i>lasA</i>	9.84 (3.49, 27.82) 0.0010	1.73 (1.04, 2.89) 0.034	0.61 (0.36, 1.05) 0.069
<i>sagS</i>	1.54 (0.91, 2.63) 0.105	2.47 (1.39, 4.39) 0.002	0.45 (0.25, 0.81) 0.006
<i>rsmY</i>	2.99 (1.61, 5.58) 0.0010	7.28 (3.28, 16.16) 0	0.18 (0.08, 0.38) <0.001
<i>rsmZ</i>	3.31 (1.72, 6.38) 0.0010	7.89 (3.44, 18.12) 0	0.14 (0.06, 0.34) <0.001
<i>pelB</i>	1020.45 (9.29, 112044.57) 0.003	1.98 (1.16, 3.36) 0.011	0.53 (0.30, 0.92) 0.021
<i>phzF</i>	2,300,401.50 (0, 18394) 0.286	2.37 (1.38, 4.06) 0.001	0.51 (0.30, 0.87) 0.011
<i>algD</i>	29.66 (5.97, 147.27) 0.0010	2.48 (1.44, 4.26) 0.001	0.49 (0.29, 0.85) 0.01

OR Odds ratio, CI Confidence intervals, CAP Community-acquired pneumonia, VAP Ventilator-associated pneumonia, HAP Hospital-acquired pneumonia

gene expression and co-infection, adverse events, or multi-drug resistance, as shown in Additional file 1 Table S5.

#### **tesG expression correlates the modulation of host inflammatory responses**

The upregulation of *tesG* expression was strongly correlated ( $P=0.001$ ;  $r<-0.8$ ) with a decrease in both systemic and sputum inflammatory responses. However, no significant negative correlation was found between *tesG* expression and CRP levels (Fig. 2). The negative correlations were found for the expression of *lasR*, *rhIA*, *lasB*, and *phzF*; in particular, the upregulation of *lasR*, *rhIA*, and *lasB* was correlated with decreased sputum eosinophil and neutrophil counts. Conversely, *sagS*, *rsmY*, and *rsmZ* exhibited a weaker negative correlation with host inflammatory markers.

#### **tesG expression was correlated with the expression of other genes and some biofilm-associated virulence factors**

*tesG* expression strongly correlated with *phzF*, *lasR*, *lasA*, *lasB*, and *rhIA* expression levels (Fig. 3) ( $P<0.0001$ ) ( $r=0.9$ ). However, no significant correlation was found between the expression of other genes. Interestingly, only the extracellular DNA (eDNA) content was significantly ( $P<0.0001$ ) ( $r=0.9$ ) correlated with *tesG*, *lasR*, *rhIA*, and *phzF* expression (Fig. 3).

Pyocyanin levels were positively correlated with increased cytotoxicity in A549 cells ( $P<0.0001$ ) ( $r>0.8$ ) (Fig. 3).

#### **The tesG expression level can predict the level of biofilm biomass**

The expression of all the genes predicted a greater proportion of the sensitivity and specificity of the biofilm structure or biomass (Fig. 4). However, *tesG*, ( $P=0.001$ ; AUC=0.9) *lasR*, ( $P=0.001$ ; AUC=0.9), and *pelB* ( $P<0.01$ ; AUC, 0.9) expression levels were accurate and sensitive for biofilm structure and biomass prediction (Fig. 4).

#### **Discussion**

Chronic *P. aeruginosa* respiratory biofilm infection is clinically considered difficult to diagnose and manage [2, 4, 6, 7, 11]. A clear clinical marker tailored to chronic *P. aeruginosa* respiratory infections has the potential to have a major impact on the implementation of adequate treatment and the patient quality of life. Here, we report the importance of analysing the expression of selected *P. aeruginosa* gene markers in human sputum samples to identify and aid in tackling the progression of chronic infections and clinical outcomes. Our results showed that clinical deterioration, inflammation in the lungs, survival, and bacterial burden are associated with distinctive bacterial gene expression patterns and consequent biofilm formation.

We observed clear, distinguishable characteristics between strong and moderate *P. aeruginosa* biofilms in the sputum of this patient cohort. In addition, a strong biofilm structure is clearly associated with clinical deterioration and subsequent risk of high mortality. Therefore, *P. aeruginosa* biofilm biomass heterogeneity directly

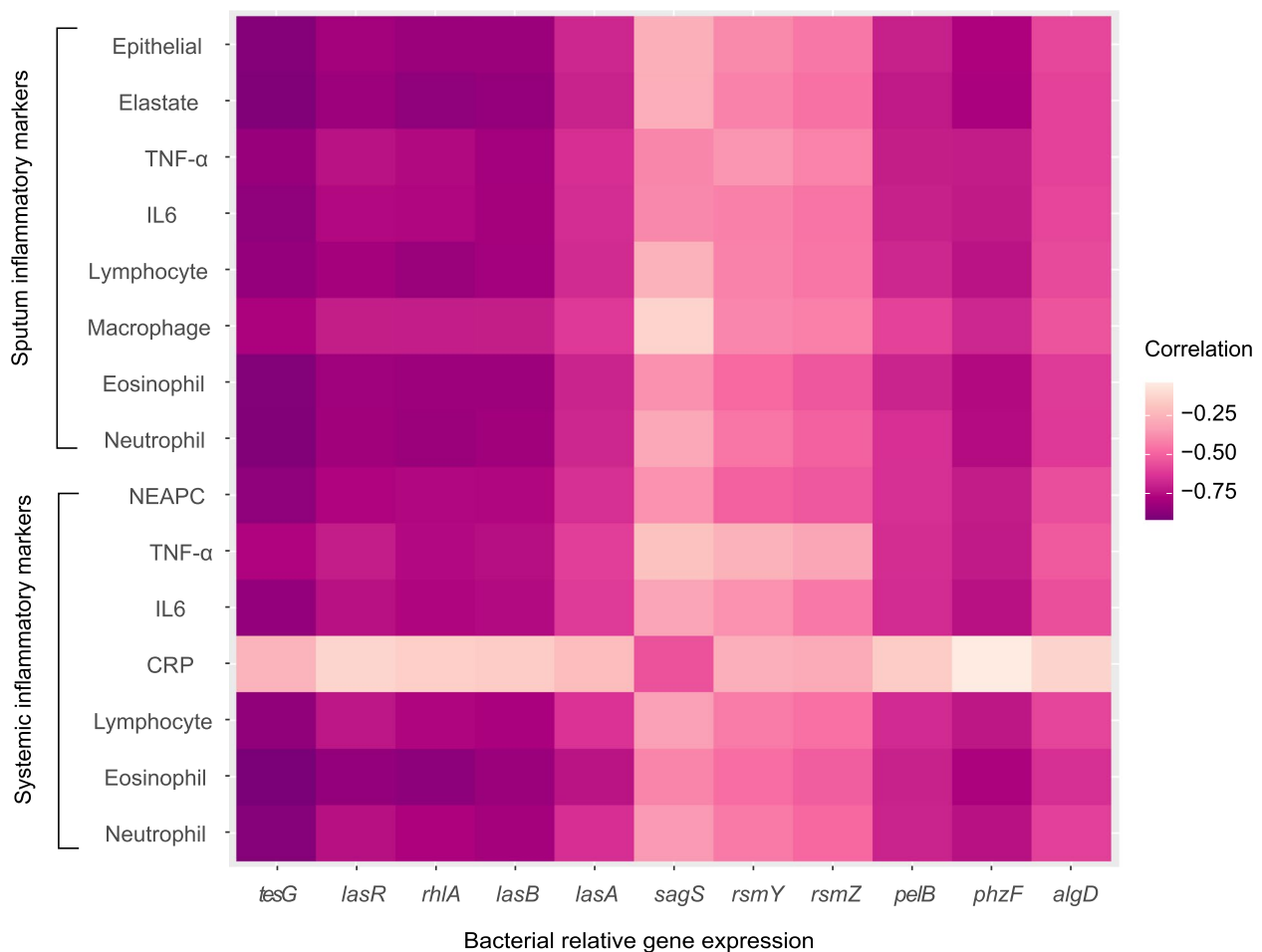


**Fig. 2** Correlation of bacterial sputum gene expression and inflammatory markers among patients with chronic *P. aeruginosa* lung infection ( $n = 70$ ). The strength of correlation is represented by the colour intensity, with darker shades indicating stronger negative correlations

impacts patient survival and the potential for antibiotic treatment failure [18]. Notably, we observed that biofilms are associated with prolonged hospitalisation and more severe cases requiring longer ICU care [1, 56]. Therefore, this approach may increase the likelihood of contracting future infections, experiencing organ failure, and the probability of developing antibiotic resistance. Furthermore, a strong biofilm structure increases *P. aeruginosa* tolerance to antibiotic therapy, increasing selective pressure on developing resistance reservoirs within the host.

In the present patient cohort, the increased incidence of pneumonia in the strong biofilm formation group was clinically important. This incidence is particularly concerning as HAP or VAP can lead to serious complications, lengthening of ICU stay, and further worsening of patient outcomes. However, this finding is different from reports that found no differences between VAP and non-VAP strains regarding biofilm production [50]. As airway bacterial colonisation and biofilm formation on

endotracheal tubes (ETTs) are early and frequent events in ventilated patients [7, 8, 57, 58], we believe that the increase in biofilm formation may be an adaptation to the mechanically ventilated environment and subsequently contribute to VAP development. While there was no significant difference in the overall incidence of co-infection between the groups, the strong biofilm formation group had a greater incidence of *A. baumannii* co-infection. This might indicate a specific vulnerability of these patients to certain pathogens. Additionally, *P. aeruginosa* biofilm infection promotes co-infection with *A. baumannii* through Psl exopolysaccharide-dependent cooperation, enhancing its interactions with *A. baumannii* and contributing to the antibiotic resistance of *P. aeruginosa* in biofilm infections [59]. Meanwhile, other *P. aeruginosa* EPS structural fibres, including eDNA, further contributed to the Psl-dependent dual-species biofilm stability under antibiotic treatment [59]. Moreover, as consistent with the findings of other studies, our patient cohort's

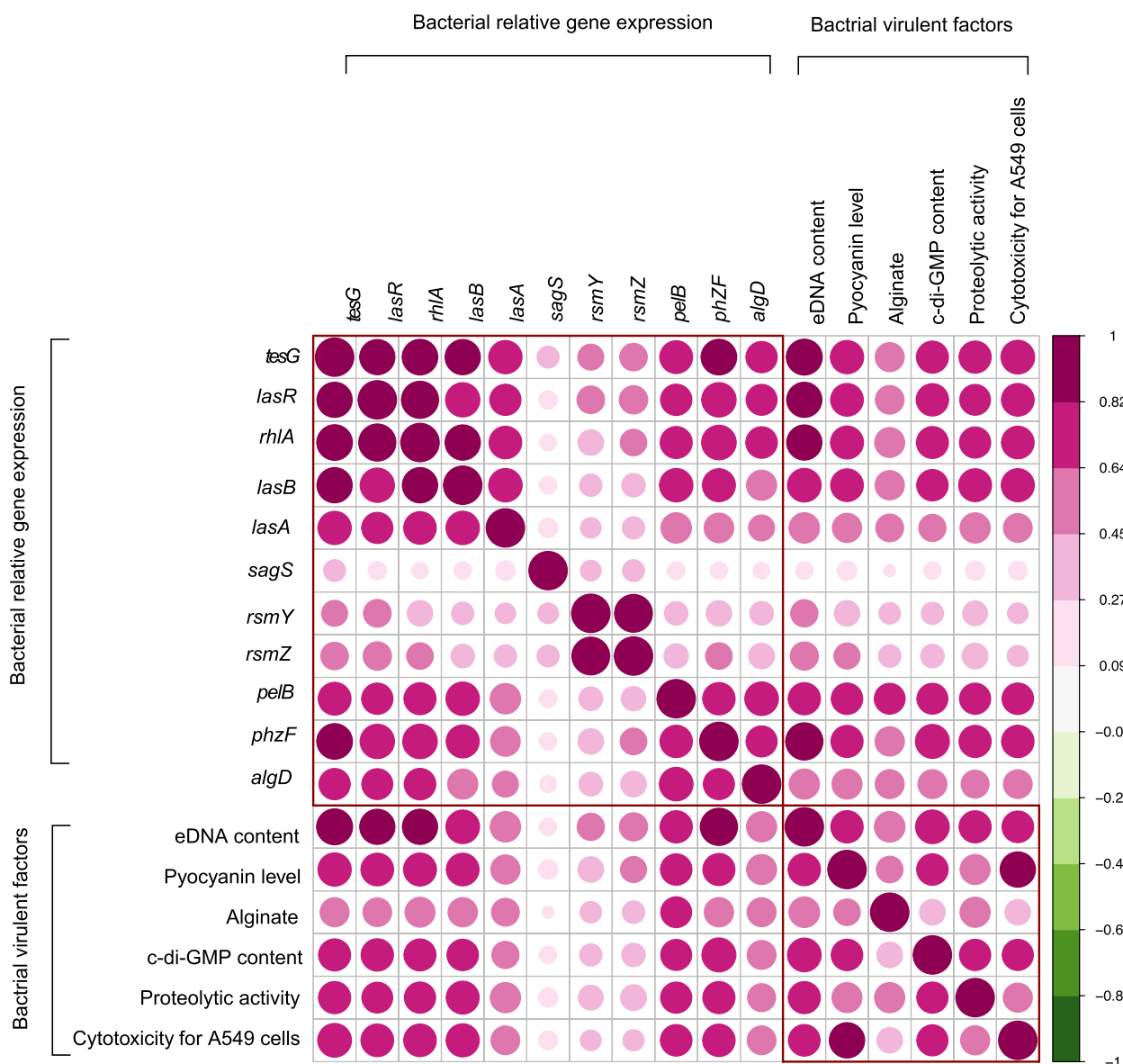


**Fig. 3** Correlation of bacterial sputum gene expression and bacterial virulence factors among patients with chronic *P. aeruginosa* lung infection ( $n = 70$ ). The intensity and size of the circles indicate the strength and direction of the correlation, with darker and larger circles representing stronger correlations. c-di-GMP: (bis-(3'-5'))-cyclic diguanosine monophosphate

inflammatory marker levels were significantly associated with clinical deterioration and risk of mortality [1, 2, 4, 14, 60] (Additional file 1 Table S2, S3 and S4).

In the present study, we found an association between the newly described *tesG*, which encodes the type I secretion effector TesG of *P. aeruginosa*, and prolonged ICU or hospitalisation days and an increased risk of death [9]. Furthermore, we observed a positive correlation between *tesG* expression and strong bio-film formation and the extracellular DNA content, a crucial component of the biofilm structure [1, 2, 28,

52]. Importantly, we found that *tesG* expression was linked to lower sputum and systemic inflammation, an elevated risk of pneumonia, and worsening of pneumonia. These results align with previous observations in mice with chronic *P. aeruginosa* lung infections that revealed a role for *tesG* in dampening the host inflammatory response and phagocytosis [9, 14]. TesG enters the intracellular compartment of macrophages through clathrin-mediated endocytosis and competitively inhibits the activity of eukaryotic small GTPases, a family of molecular switches that regulate critical cellular

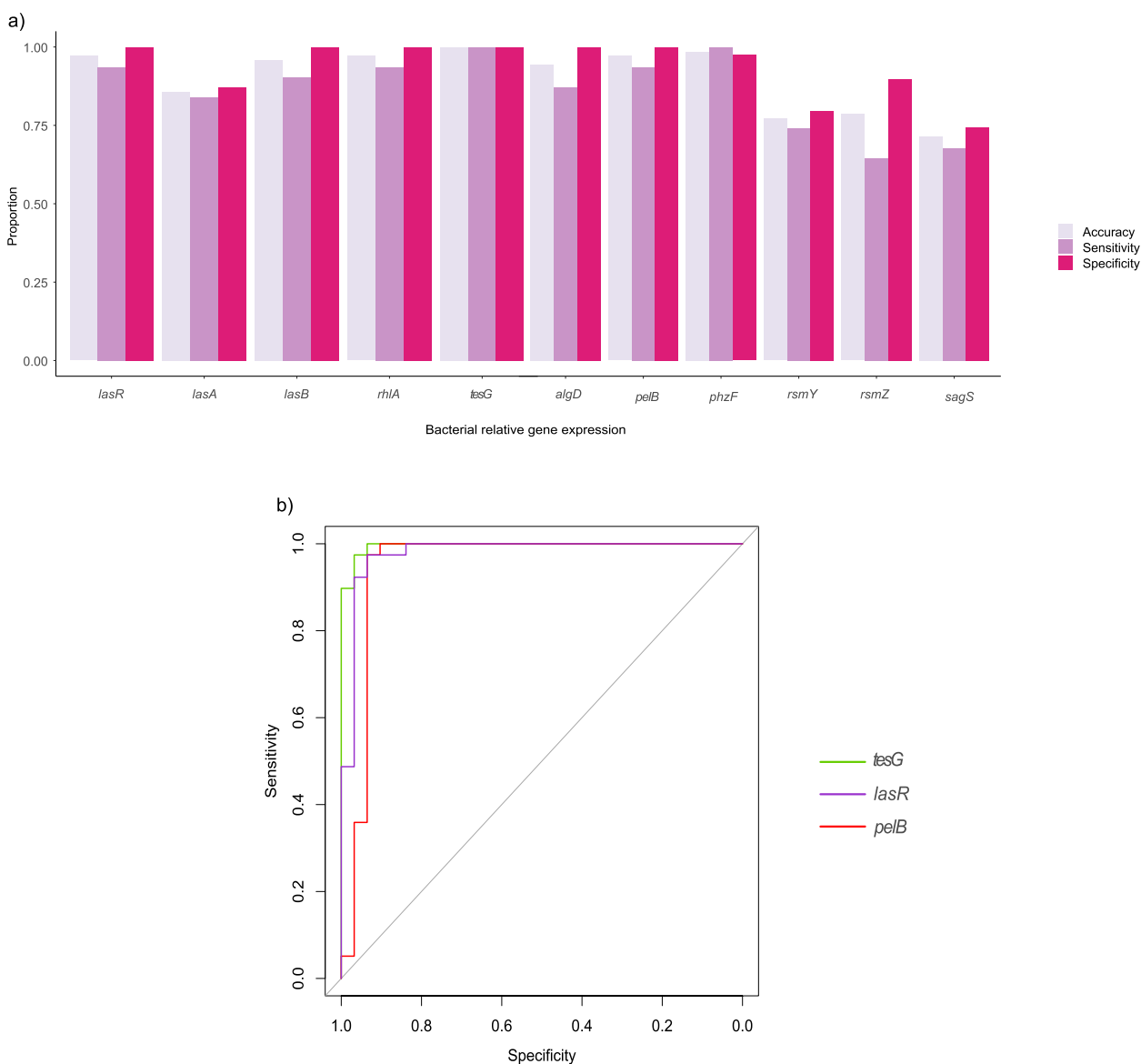


**Fig. 4** **a** Relationship of bacterial sputum gene expression in terms of predicting biofilm biomass and **b** receiver operating characteristic (ROC) curve for *lasR*, *pelB*, and *tesG* sputum expression in terms of predicting biofilm biomass among patients with chronic *P. aeruginosa* lung infection (n = 70)

processes [9]. Small GTPases are essential for neutrophil chemotaxis, motility, and recruitment to infection sites [61]. By interfering with their function, TesG suppresses neutrophil influx, weakening the host’s immune response. Additionally, this inhibition disrupts cytoskeletal rearrangement in macrophages, impairing their ability to engulf bacteria through phagocytosis. TesG also reduces the production and release of cytokines and chemokines, further dampening the inflammatory response and facilitating bacterial survival and persistence [9].

Our clinical findings echo observations in mouse models [9], revealing that TesG can facilitate the development of chronic lung infection, leading to lower survival rates and greater bacterial burdens. To our knowledge, we are the first to validate such a relationship clinically. TesG is regulated by the vital quorum-sensing system and is secreted by the downstream type I secretion system [9]. We also observed that *tesG* is correlated with the quorum-sensing genes *lasR*, *rhlA*, *lasB*, and *lasA*. Quorum-sensing genes favour strong biofilm formation and clinical worsening of in patients [2, 5, 9, 10, 14], a

correlation that was further confirmed by our findings. In addition, the observation that *tesG* is correlated with quorum-sensing genes suggests that *TesG* may either directly influence quorum sensing, enhancing biofilm-related gene expression, or be co-regulated with these genes, thereby amplifying the effects of the quorum-sensing system. Consequently, the combined activity of *tesG* and these quorum-sensing genes may contribute to increased biofilm biomass.

Therefore, in addition to affecting the host and inhibiting cellular functions designed to protect the host, including inflammation and phagocytosis, *tesG* may contribute to biofilm production through the quorum-sensing pathway.

Moreover, the expression of *tesG* correlates with the expression of *PhzF*, which catalyses the first step in the biosynthesis of phenazine-1-carboxylic acid, pyocyanin, and other phenazines [62]. Redox-active pyocyanin is a toxic secondary metabolite secreted by *P. aeruginosa* that modulates mucin glycosylation via sialyl-Lewis<sup>x</sup> to increase binding to airway epithelial cells [63]. Although we found that pyocyanin levels significantly affected prolonged clinical worsening in patients (Additional file Table S2, S3 and S4), we did not observe a significant correlation between *tesG* and pyocyanin levels. This discrepancy may be attributed to the complex biosynthetic pathway of *P. aeruginosa* [21, 51, 62, 63]. Moreover, we also discovered that *algD* expression, which regulates alginate production [64], is directly related to the clinical deterioration of patients and biofilm formation. This deterioration may be due to the alginate produced by mucoid *P. aeruginosa* being sufficient to inhibit alveolar macrophage efferocytosis and airway inflammation [64, 65]. Supporting this hypothesis is the observation of higher levels of alginate in people with bronchiectasis, CF, or the “exacerbator” COPD phenotype [1, 2, 4, 7, 64, 65]. As *tesG* and *algD* affect alveolar macrophage function [9, 64, 65], interestingly, we found no significant correlation between *tesG* and *algD* expression levels. Moreover, *rsmY* and *rsmZ*, small noncoding regulatory RNAs [66] in *P. aeruginosa* also significantly promoted prolonged clinical worsening in our patient cohort. The *rsmY* and *rsmZ* regulate *RsmA*, and possibly *RsmF*, a family of RNA-binding proteins that regulate protein synthesis at the posttranscriptional level [66]. Opportunistic pathogens such as *P. aeruginosa* use *RsmA* and *RsmF* to regulate factors inversely associated with acute and chronic virulence phenotypes [66]. Notably, we did not find a significant correlation between *tesG* and the *rsmY* or *rsmZ* expression levels. Therefore, we hypothesise that *P. aeruginosa* *tesG* expression is an independent pathway of the biosynthesis of other virulence factors. However, by acting altogether, these regulatory genes

help *P. aeruginosa* to successfully establish chronic biofilm infections, co-regulating this establishment with other virulence factors. This expression ultimately leads to poor prognosis, significant physical impairment, and mortality.

Although our findings are drawn from a limited sample size, our sample set is more coherent and structured than that used in any previous study. A broader clinical cohort could further validate the observed associations. Additionally, host microbiome factors that may influence biofilm formation, inflammation, and clinical outcomes were not fully explored. Although no correlation was identified between the tested genes and MDR *P. aeruginosa*, the possibility of indirect or complex interactions affecting antibiotic resistance mechanisms remains an area for further investigation.

To our knowledge, this is the first clinical study to examine how novel *tesG* gene expression is associated with chronic *P. aeruginosa* respiratory biofilm infections and how the extent of biofilm infections affects the clinical deterioration of the patients. We provide data covering most aspects of the impact of chronic *P. aeruginosa* chronic biofilm lung infection on patients. As *P. aeruginosa* infection evolves, progressing from early to intermittent and then chronic infection [1, 2, 4], we hypothesise that the modulation of inflammation by *tesG* plays an essential role in hampering the host’s ability to prevent the establishment of chronic biofilm infection. *tesG* is unique not only because it is linked to biofilm infection but also because it is associated with modulating inflammation within the host. Unfortunately, none of the genes tested correlated with multi-drug resistance in *P. aeruginosa*. This is another example of this phenomenon, highlighting that opportunistic pathogens, such as *P. aeruginosa*, utilise multiple regulatory networks to adapt and survive within the human host. In doing so, biofilms provide *P. aeruginosa* with structural tolerance to antibiotics and immune cells, in addition to the presence of antibiotic-resistance genes. We also observed that while *lasR* and *pelB* are potential biomarkers for predicting biofilm biomass levels, their least association with inflammation reduces their appeal in the context of biofilm infections. In contrast, *tesG* demonstrates a stronger link to both biofilm formation and inflammatory processes, making it a more compelling focus for understanding and addressing biofilm infections. Moreover, *tesG* demonstrates a strong association with multiple virulence factors, including extracellular DNA content and other key biofilm-associated genes, highlighting its involvement in the structural integrity of biofilms. While some genes, such as *sagS*, have been linked to a reduced risk of mortality, *tesG* is consistently associated with worse clinical

outcomes, including pneumonia progression. This dual role in promoting biofilm stability while dampening host immune responses suggests that *tesG* plays a critical role in the transition from acute to chronic infection, making it a valuable biomarker for disease severity and a potential target for therapeutic intervention.

## Conclusions

In conclusion, our study provides a useful clinical explanation for the importance of *tesG* expression during chronic pseudomonal lung infections. Among the biofilm-associated genes examined, *tesG* stands out as a key gene in *P. aeruginosa* infections due to its multifaceted role in biofilm formation, host immune modulation, and clinical severity. Unlike other genes that contribute to biofilm structure, *tesG* is uniquely linked to both biofilm development and the regulation of inflammatory responses, suggesting a broader impact on infection dynamics. Its expression correlates with prolonged hospitalisation, ICU stay, and disease progression, reinforcing its role in severe and persistent infections. We also highlighted the potential of *tesG* gene expression as a prognostic biomarker of chronic biofilm infection, which could lead to appropriate clinical management actions at the appropriate time. Furthermore, quorum-sensing-mediated *tesG* gene expression may also reveal promising targets for developing anti-biofilm drugs and pave the way for more effective clinical therapy for chronic infections.

## Abbreviations

CAP	Community-acquired pneumonia
CDI	Contact-dependent growth inhibition
c-di-GMP	Cyclic bis-(3',5')-dimeric guanosine monophosphate
CF	Cystic fibrosis
CLSI	Clinical and Laboratory Standards Institute
CLSM	Confocal laser scanning microscopy
COPD	Chronic obstructive pulmonary disease
CRP	C-reactive protein
DCC	Differential cell count
DMEM	Dulbecco's modified Eagle's medium
DNA	Deoxyribonucleic acid
ETTs	Endotracheal tubes
EUCAST	The European Committee on Antimicrobial Susceptibility Testing
FEV1	Ratio of forced expiratory volume in one second to forced vital capacity
FISH	Fluorescence in situ hybridisation
FVC	Forced vital capacity
HAP	Hospital-acquired pneumonia
LCMS	Liquid chromatography–mass spectrometry
LOHS	Length of hospital stays
LOICU	Length of intensive care unit stays
MDR	Multidrug resistant
PNA	Peptide nucleic acid
QS	Quorum-sensing
RNA	Ribonucleic acid
TCA	Trichloroacetic acid
VAP	Ventilator-associated pneumonia

## Supplementary Information

The online version contains supplementary material available at <https://doi.org/10.1186/s12916-025-04009-x>.

Additional file 1: Methods - Müller-Hinton broth composition, Minimal inhibitory concentrations for planktonic cells, m-hydroxydiphenyl method, cDNA synthesis, Ethanol precipitation, Results - Association of inflammatory markers and bacterial virulence factors with hospital/ICU stay and mortality, Associations between biofilm structure, inflammatory markers, lung function, and bacterial virulence factors, Table S1-S6. Table S1- List of Primers. Table S2 - Relationships between systemic inflammatory markers or sputum inflammatory markers or bacteria virulence factors and length of hospital stay (LOHS), length of ICU stay (LOICU) and mortality in patients with chronic *P. aeruginosa* lung infection ( $n = 70$ ) based on the odd ratio (OR) adjusted for sex and age.  $P < 0.05$  was considered to indicate significance. Table S3 - Relationships between systemic inflammatory markers or sputum inflammatory markers or bacteria virulence factors and biofilm Structure, HAP, VAP or CAP, pneumonia status within 7 days in patients with chronic *P. aeruginosa* lung infection ( $n = 70$ ) based on the odd ratio (OR) adjusted for sex and age.  $P < 0.05$  was considered to indicate significance. Table S4- Relationships between gene expression or systemic inflammatory markers or sputum inflammatory markers or bacteria virulence and adverse events, multidrug resistance, Co-infections in patients with chronic *P. aeruginosa* lung infection ( $n = 70$ ) based on the odd ratio (OR) adjusted for sex and age.  $P < 0.05$  was considered to indicate significance. Table S5 - Antibiotic resistance as a percentage (%) in patients with chronic *P. aeruginosa* lung infection ( $n = 70$ ). Table S6 - Sputum RNA concentration

Additional file 2.

## Acknowledgements

We thank the staff of the bacteriology division, Department of Microbiology at King Chulalongkorn Memorial Hospital, for providing the *P. aeruginosa* clinical isolates and sputum samples. We, the authors of this paper, embrace inclusive, diverse, and equitable conduct of research. Our team comprises individuals who self-identify as underrepresented ethnic minorities, gender minorities, members of the LGBTQIA+ community, and individuals living with disabilities. We actively promote gender balance in our reference list while maintaining scientific relevance. The authors of this paper, embrace inclusive, diverse, and equitable conduct of research. Our team comprises individuals who self-identify as underrepresented ethnic minorities, gender minorities, members of the LGBTQIA+ community, and individuals living with disabilities. We actively promote a gender balance in our reference list while maintaining scientific relevance.

## Data visualisation

The data were visualised using ggplot2 3.3.5, a package of R programme version 4.1.0 [55].

## Authors' contributions

D.L.W., C.H., and P.H. conceived the study, acquired funding, and conducted the investigation, data curation, formal analysis, and writing of the original draft. D.L.W. and P.G.H. contributed equally to this work as first authors. Clinical data collection was conducted by P.T., K.J., S.L., S.N., U.R., and C.T. P.N.M., G.H., W.G.F.D., P.P., P.O., K.M., L.C., N.K.D.R., S.M.A.H.R., A.K1., R.J.S., H.I., M.A., S.C., A.L., T.K., J.D., S.M.S., A.K2., T.C., S.A., and K.S. provided supervision, critical review, and manuscript editing. D.L.W., C.H., and P.P. directly accessed and verified the underlying data. All authors reviewed and approved the final manuscript.

## Authors' Twitter handles

@dr\_leshan, @DrAnthonyKicic, @stephen\_stick, @AishaKhatib.

## Funding

This work was supported by a grant from the 90th Year Anniversary Ratchadapiseksompotch Endowment Fund from the Faculty of Medicine and Graduate School, Chulalongkorn University, Bangkok, Thailand (batch No. 39 (2/61)). Dhammika Leshan Wannigama was supported by Chulalongkorn University (Second Century Fund- C2F Fellowship), the University of Western Australia

(Overseas Research Experience Fellowship) and Yamagata Prefectural Central Hospital, Yamagata, Japan (Clinical Residency Fellowship). Anthony Kicic is a Rothwell Family Fellow. Jane Davies is funded by grants from the Cystic Fibrosis Trust and supported by the National Institute for Health and Care Research through the Imperial Biomedical Research Centre and a Senior Investigator Award. The sponsor(s) had no role in the study design; in the collection, analysis, or interpretation of the data; in the writing of the report; or in the decision to submit the article for publication.

#### Data availability

This published article and its Additional file 1 includes data generated and analyzed during this study. The additional de-identified participant clinical data will be available upon reasonable request from the corresponding author DLW. The RT-qPCR data is available through Harvard Dataverse: <https://doi.org/10.7910/DVN/3WST4A>. Qualified external researchers only can access the data, and types of analysis requests are at the research team's discretion and dependent on the nature of the request, the merit of the research proposed, the availability of the data, and the intended use of the data. Mechanisms of data availability will be with a signed data access agreement. The requested proposal must include a statistician.

#### Declarations

##### Ethics approval and consent to participate

The study protocol was approved (IRB No. 414/60) by the Institutional Review Board of the Faculty of Medicine, Chulalongkorn University, Bangkok, Thailand, and was performed in accordance with the ethical standards as established in the 1964 Declaration of Helsinki and its later amendments and comparable ethical standards.

For this retrospective, non-interventional study of pseudonymised clinical isolates, the requirement for informed consent from patients was waived by the Institutional Review Board (IRB No. 414/60) of the Faculty of Medicine, Chulalongkorn University, Bangkok, Thailand.

##### Competing interests

The authors declare no competing interests.

##### Author details

<sup>1</sup>Department of Infectious Diseases and Infection Control, Yamagata Prefectural Central Hospital, Yamagata, Japan. <sup>2</sup>Department of Microbiology, Faculty of Medicine, Chulalongkorn University, King Chulalongkorn Memorial Hospital, Thai Red Cross Society, 1873 Rama 4 Road, Bangkok, Pathumwan, Thailand. <sup>3</sup>Center of Excellence in Antimicrobial Resistance and Stewardship Research, Faculty of Medicine, Chulalongkorn University, Bangkok, Thailand. <sup>4</sup>School of Medicine, Faculty of Health and Medical Sciences, The University of Western Australia, Nedlands, WA, Australia. <sup>5</sup>Biofilms and Antimicrobial Resistance Consortium of ODA Receiving Countries, the University of Sheffield, Sheffield, UK. <sup>6</sup>Pathogen Hunter's Research Team, Department of Infectious Diseases and Infection Control, Yamagata Prefectural Central Hospital, Yamagata, Japan. <sup>7</sup>Department of Infectious Diseases, Faculty of Medicine, Yamagata University and Yamagata University Hospital, Yamagata, Japan. <sup>8</sup>Department of Clinical Epidemiology, Faculty of Medicine, Thammasat University, Rangsit, Thailand. <sup>9</sup>Biostatistics Group, QIMR Berghofer Medical Research Institute, Brisbane, QLD, Australia. <sup>10</sup>Center of Excellence in Applied Epidemiology, Thammasat University, Rangsit 10120, Thailand. <sup>11</sup>Mater Research Institute, University of Queensland, Queensland, Australia. <sup>12</sup>Department of Infection, Immunity & Cardiovascular Disease, University of Sheffield Medical School, Sheffield, UK. <sup>13</sup>Faculty of Health Science Technology, Chulabhorn Royal Academy, Bangkok 10210, Thailand. <sup>14</sup>HRH Princess Chulabhorn Disaster and Emergency Medicine Center, Chulabhorn Royal Academy, Bangkok 10210, Thailand. <sup>15</sup>Department of Biology, Faculty of Science, Mahidol University, Bangkok, Thailand. <sup>16</sup>Department of Medicine, Faculty of Medicine, Chulalongkorn University and King Chulalongkorn Memorial Hospital, Bangkok, Thailand. <sup>17</sup>Department of Clinical Microbiology and Applied Technology, Faculty of Medical Technology, Mahidol University, Bangkok, Thailand. <sup>18</sup>Division of Bacteriology, School of Medicine, Jichi Medical University, Tochigi, Japan. <sup>19</sup>Department of Chemical and Biological Engineering, The University of Sheffield, Sheffield, UK. <sup>20</sup>Department of Clinical Microbiology, Christian Medical College, Vellore, India. <sup>21</sup>Department of Microbiology and Immunology, University of Otago, Dunedin, Otago 9010, New Zealand. <sup>22</sup>Center of Excellence

in Immunology and Immune-Mediated Diseases, Chulalongkorn University, Bangkok 10330, Thailand. <sup>23</sup>Department of Family & Community Medicine, University of Toronto, Toronto, ON, Canada. <sup>24</sup>Office of Graduate Affairs, Faculty of Medicine, Chulalongkorn University, Bangkok, Thailand. <sup>25</sup>Yamagata Prefectural University of Health Sciences, Kamiyanagi, Yamagata 990-2212, Japan. <sup>26</sup>Department of Civil and Environmental Engineering, Graduate School of Engineering, Tohoku University, Miyagi, Japan. <sup>27</sup>Department of Anesthesiology, Faculty of Medicine, King Chulalongkorn Memorial Hospital, Thai Red Cross Society, Chulalongkorn University, Bangkok, Thailand. <sup>28</sup>Translational Research in Inflammation and Immunology Research Unit (TRIRU), Department of Microbiology, Chulalongkorn University, Bangkok, Thailand. <sup>29</sup>Division of Nephrology, Department of Medicine, Faculty of Medicine, Chulalongkorn University, Bangkok, Thailand. <sup>30</sup>Center of Excellence in Kidney Metabolic Disorders, Faculty of Medicine, Chulalongkorn University, Bangkok, Thailand. <sup>31</sup>Dialysis Policy and Practice Program (Dip3), School of Global Health, Faculty of Medicine, Chulalongkorn University, Bangkok, Thailand. <sup>32</sup>Peritoneal Dialysis Excellence Center, King Chulalongkorn Memorial Hospital, Bangkok, Thailand. <sup>33</sup>Institute for Medical Microbiology, Immunology and Hygiene, Faculty of Medicine University Hospital Cologne, University of Cologne, Cologne, Germany. <sup>34</sup>German Centre for Infection Research, Partner Site Bonn-Cologne, Cologne, Germany. <sup>35</sup>National Heart and Lung Institute, Imperial College London, London, UK. <sup>36</sup>Department of Paediatric Respiratory Medicine, Royal Brompton Hospital, London, UK. <sup>37</sup>Centre for Cell Therapy and Regenerative Medicine, Medical School, The University of Western Australia, Nedlands, WA 6009, Australia. <sup>38</sup>Department of Respiratory and Sleep Medicine, Perth Children's Hospital, Nedlands, WA 6009, Australia. <sup>39</sup>Wal-Yan Respiratory Research Centre, Telethon Kids Institute, University of Western Australia, Nedlands, WA 6009, Australia. <sup>40</sup>School of Population Health, Curtin University, Bentley, WA 6102, Australia. <sup>41</sup>Tokyo Foundation for Policy Research, Minato-Ku, Tokyo, Japan.

Received: 15 April 2024 Accepted: 13 March 2025

Published online: 31 March 2025

#### References

- Maurice NM, Bedi B, Sadikot RT. Pseudomonas aeruginosa Biofilms: Host Response and Clinical Implications in Lung Infections. *Am J Respir Cell Mol Biol*. 2018;58(4):428–39.
- Rossi E, La Rosa R, Bartell JA, Marvig RL, Haagensen JAJ, Sommer LM, et al. Pseudomonas aeruginosa adaptation and evolution in patients with cystic fibrosis. *Nat Rev Microbiol*. 2021;19(5):331–42.
- Gaibani P, Viciani E, Bartoletti M, Lewis RE, Tonetti T, Lombardo D, et al. The lower respiratory tract microbiome of critically ill patients with COVID-19. *Sci Rep*. 2021;11(1):10103.
- Faure E, Kwong K, Nguyen D. Pseudomonas aeruginosa in chronic lung infections: how to adapt within the host? *Front Immunol*. 2018;9:2416.
- Folkesson A, Jelsbak L, Yang L, Johansen HK, Ciofu O, Høiby N, et al. Adaptation of Pseudomonas aeruginosa to the cystic fibrosis airway: an evolutionary perspective. *Nat Rev Microbiol*. 2012;10(12):841–51.
- Martínez-Solano L, Macía MD, Fajardo A, Oliver A, Martínez JL. Chronic pseudomonas aeruginosa infection in chronic obstructive pulmonary disease. *Clin Infect Dis*. 2008;47(12):1526–33.
- García-Clemente M, de la Rosa D, Máz L, Girón R, Blanco M, Oliveira C, et al. Impact of pseudomonas aeruginosa infection on patients with chronic inflammatory airway diseases. *J Clin Med*. 2020;9(12):3800.
- Murphy TF, Brauer AL, Eschberger K, Lobbins P, Grove L, Cai X, et al. Pseudomonas aeruginosa in chronic obstructive pulmonary disease. *Am J Respir Crit Care Med*. 2008;177(8):853–60.
- Zhao K, Li W, Li J, Ma T, Wang K, Yuan Y, et al. TesG is a type I secretion effector of Pseudomonas aeruginosa that suppresses the host immune response during chronic infection. *Nat Microbiol*. 2019;4(3):459–69.
- Feliziani S, Luján AM, Moyano AJ, Sola C, Bocco JL, Montanaro P, et al. Mucoicid, quorum sensing, mismatch repair and antibiotic resistance in Pseudomonas aeruginosa from cystic fibrosis chronic airways infections. *PLoS One*. 2010;5(9):e12669.
- Araújo D, Shteinberg M, Aliberti S, Goeminne PC, Hill AT, Fardon TC, et al. The independent contribution of Pseudomonas aeruginosa infection to long-term clinical outcomes in bronchiectasis. *Eur Respir J*. 2018;51(2):1701953.

12. Barthe C, Nandakumar S, Derlich L, Macey J, Bui S, Fayon M, et al. Exploring the expression of *Pseudomonas aeruginosa* genes directly from sputa of cystic fibrosis patients. *Lett Appl Microbiol*. 2015;61(5):423–8.
13. Pincus NB, Ozer EA, Allen JP, Nguyen M, Davis JJ, Winter DR, et al. A genome-based model to predict the virulence of *Pseudomonas aeruginosa* isolates. *mBio*. 2020;11(4):e01527–20. <https://doi.org/10.1128/mBio.01527-20>.
14. Filloux A, Davies JC. Chronic infection by controlling inflammation. *Nat Microbiol*. 2019;4(3):378–9.
15. Allen JP, Ozer EA, Minasov G, Shuvalova L, Kiryukhina O, Anderson WF, et al. A comparative genomics approach identifies contact-dependent growth inhibition as a virulence determinant. *Proc Natl Acad Sci*. 2020;117(12):6811–21.
16. Shao X, Yao C, Ding Y, Hu H, Qian G, He M, et al. The transcriptional regulators of virulence for *Pseudomonas aeruginosa*: Therapeutic opportunity and preventive potential of its clinical infections. *Genes & Diseases*. 2023;10(5):2049–63.
17. Qin S, Xiao W, Zhou C, Pu Q, Deng X, Lan L, et al. *Pseudomonas aeruginosa*: pathogenesis, virulence factors, antibiotic resistance, interaction with host, technology advances and emerging therapeutics. *Signal Transduct Target Ther*. 2022;7(1):199.
18. Wannigama DL, Hurst C, Hongsing P, Pearson L, Saethang T, Chantavisoot N, et al. A rapid and simple method for routine determination of antibiotic sensitivity to biofilm populations of *Pseudomonas aeruginosa*. *Ann Clin Microbiol Antimicrob*. 2020;19(1):8.
19. Rossi E, Falcone M, Molin S, Johansen HK. High-resolution in situ transcriptomics of *Pseudomonas aeruginosa* unveils genotype independent patho-phenotypes in cystic fibrosis lungs. *Nat Commun*. 2018;9(1):3459.
20. Fothergill JL, Neill DR, Loman N, Winstanley C, Kadiloglu A. *Pseudomonas aeruginosa* adaptation in the nasopharyngeal reservoir leads to migration and persistence in the lungs. *Nat Commun*. 2014;5(1):4780.
21. Wu D, Huang W, Duan Q, Li F, Cheng H. Sodium houthuyfonate affects production of N-acyl homoserine lactone and quorum sensing-regulated genes expression in *Pseudomonas aeruginosa*. *Front Microbiol*. 2014;5:635.
22. Petrova OE, Sauer K. *SagS* Contributes to the Motile-Sessile Switch and Acts in Concert with *BfSR* To Enable *Pseudomonas aeruginosa* Biofilm Formation. *J Bacteriol*. 2011;193(23):6614–28.
23. Pfaffl MW. A new mathematical model for relative quantification in real-time RT-PCR. *Nucleic Acids Res*. 2001;29(9):e45.
24. EUCAST ECoAST- Clinical breakpoints - bacteria (v 12.0). European Committee on Antimicrobial Susceptibility Testing. 2022;12.
25. Institute CaS. Performance Standards for Antimicrobial Susceptibility Testing, 32nd Edition. 2022;32:362.
26. Lopes SP, Azevedo NF, Pereira MO. Quantitative assessment of individual populations within polymicrobial biofilms. *Sci Rep*. 2018;8(1):9494.
27. Moser C, Van Gennip M, Bjarnsholt T, Jensen P, Lee B, Hougen HP, et al. Novel experimental *Pseudomonas aeruginosa* lung infection model mimicking long-term host-pathogen interactions in cystic fibrosis. *APMIS*. 2009;117(2):95–107.
28. Phuengmaung P, Somparn P, Panpetch W, Singkham-In U, Wannigama DL, Chatsuwat T, et al. Coexistence of *Pseudomonas aeruginosa* with *Candida albicans* enhances biofilm thickness through alginate-related extracellular matrix but is attenuated by n-acetyl-L-cysteine. *Front Cell Infect Microbiol*. 2020;10:594336.
29. Wannigama DL, Hurst C, Pearson L, Saethang T, Singkham-in U, Luk-in S, et al. Simple fluorometric-based assay of antibiotic effectiveness for *Acinetobacter baumannii* biofilms. *Sci Rep*. 2019;9(1):6300.
30. Hongsing P, Kongart C, Nuiden N, Wannigama DL, Phairoh K. Quantitative analysis of swertiamarin content from *Fragaria fragrans* leaf extract using HPLC technique and its correlation to antibacterial activity. *J Curr Sci Technol*. 2024;14(2):34.
31. Wannigama DL, Dwivedi R, Zahraei-Ramazani A. Prevalence and Antibiotic Resistance of Gram-Negative Pathogenic Bacteria Species Isolated from *Periplaneta americana* and *Blattella germanica* in Varanasi. *India J Arthropod Borne Dis*. 2014;8(1):10–20.
32. Devanga Ragupathi NK, Muthuirulandi Sethuvel DP, Ganesan A, Murugan D, Baskaran A, Wannigama DL, et al. Evaluation of *mrkD*, *pgaC* and *wcaJ* as biomarkers for rapid identification of *K. pneumoniae* biofilm infections from endotracheal aspirates and bronchoalveolar lavage. *Sci Rep*. 2024;14(1):23572.
33. Keeratikunakorn K, Kaeoket K, Ounjai P, Wannigama DL, Chatsuwat T, Ngamwongsatit N. First detection of multidrug-resistant and toxigenic *Pasteurella aerogenes* in sow vaginal discharge: a novel threat to swine health in Thailand. *Sci Rep*. 2024;14(1):25510.
34. Sutnu N, Chanchaoenthana W, Kamolratanakul S, Phuengmaung P, Singkham-In U, Chongrak C, et al. Bacteriophages isolated from mouse feces attenuates pneumonia mice caused by *Pseudomonas aeruginosa*. *PLoS ONE*. 2024;19(7):e0307079.
35. Hongsing P, Ngamwongsatit N, Kongart C, Nuiden N, Phairoh K, Wannigama DL. Cannabidiol Demonstrates Remarkable Efficacy in Treating Multidrug-Resistant *Enterococcus Faecalis* Infections In Vitro and In Vivo. *Trends in Sciences*. 2024;21(9):8150.
36. Shein AMS, Wannigama DL, Hurst C, Monk PN, Amarasiri M, Wongsurawat T, et al. Phage cocktail amikacin combination as a potential therapy for bacteremia associated with carbapenemase producing colistin resistant *Klebsiella pneumoniae*. *Sci Rep*. 2024;14(1):28992.
37. Wannigama DL, Sithu Shein AM, Hurst C, Monk PN, Hongsing P, Phatharapornjaroen P, et al. Ca-EDTA restores the activity of ceftazidime-avibactam or aztreonam against carbapenemase-producing *Klebsiella pneumoniae* infections. *iScience*. 2023;26(7):107215.
38. Shein AMS, Wannigama DL, Hurst C, Monk PN, Amarasiri M, Badavath VN, et al. Novel intranasal phage-CaEDTA-ceftazidime/avibactam triple combination therapy demonstrates remarkable efficacy in treating *Pseudomonas aeruginosa* lung infection. *Biomed Pharmacother*. 2023;168:115793.
39. Srisakul S, Wannigama DL, Higgins PG, Hurst C, Abe S, Hongsing P, et al. Overcoming addition of phosphoethanolamine to lipid A mediated colistin resistance in *Acinetobacter baumannii* clinical isolates with colistin-sulbactam combination therapy. *Sci Rep*. 2022;12(1):11390.
40. Shein AMS, Wannigama DL, Higgins PG, Hurst C, Abe S, Hongsing P, et al. High prevalence of *mgrB*-mediated colistin resistance among carbapenem-resistant *Klebsiella pneumoniae* is associated with biofilm formation, and can be overcome by colistin-EDTA combination therapy. *Sci Rep*. 2022;12(1):12939.
41. Kueakulpattana N, Wannigama DL, Luk-in S, Hongsing P, Hurst C, Badavath VN, et al. Multidrug-resistant *Neisseria gonorrhoeae* infection in heterosexual men with reduced susceptibility to ceftriaxone, first report in Thailand. *Sci Rep*. 2021;11(1):21659.
42. Shein AMS, Wannigama DL, Higgins PG, Hurst C, Abe S, Hongsing P, et al. Novel colistin-EDTA combination for successful eradication of colistin-resistant *Klebsiella pneumoniae* catheter-related biofilm infections. *Sci Rep*. 2021;11(1):21676.
43. Luk-in S, Chatsuwat T, Kueakulpattana N, Rirerm U, Wannigama DL, Plongla R, et al. Occurrence of *mcr*-mediated colistin resistance in *Salmonella* clinical isolates in Thailand. *Sci Rep*. 2021;11(1):14170.
44. Singkham-in U, Higgins PG, Wannigama DL, Hongsing P, Chatsuwat T. Rescued chlorhexidine activity by resveratrol against carbapenem-resistant *Acinetobacter baumannii* via down-regulation of *AdeB* efflux pump. *PLoS ONE*. 2020;15(12):e0243082.
45. Phuengmaung P, Somparn P, Panpetch W, Singkham-In U, Wannigama DL, Chatsuwat T, et al. Coexistence of *Pseudomonas aeruginosa* with *Candida albicans* enhances biofilm thickness through alginate-related extracellular matrix but is attenuated by n-acetyl-L-cysteine. *Front Cell Infect Microbiol*. 2020;10:594336.
46. MUsken M, Di Fiore S, Römmling U, Häussler S. A 96-well-plate–based optical method for the quantitative and qualitative evaluation of *Pseudomonas aeruginosa* biofilm formation and its application to susceptibility testing. *Nat Protoc*. 2010;5(8):1460–9.
47. Wannigama DL, Shein AMS, Hurst C, Monk PN, Hongsing P, Phatharapornjaroen P, et al. Ca-EDTA restores the activity of Ceftazidime-Avibactam or Aztreonam against carbapenemase-producing *Klebsiella pneumoniae* infections. *iScience*. 2023;26(7):107215.
48. Hongsing P, Ngamwongsatit N, Kongart C, Nuiden N, Phairoh K, Wannigama DL. Cannabidiol demonstrates remarkable efficacy in treating multidrug-resistant *enterococcus faecalis* infections in vitro and in vivo. *Trends Sci*. 2024;21(12):8150.
49. Vásquez-Ponce F, Higuera-Llantén S, Pavlov MS, Ramírez-Orellana R, Marshall SH, Olivares-Pacheco J. Alginate overproduction and biofilm formation by psychrotolerant *Pseudomonas mandelii* depend on temperature in Antarctic marine sediments. *Electron J Biotechnol*. 2017;28:27–34.

50. Alonso B, Fernández-Barat L, Di Domenico EG, Marín M, Cercenado E, Merino I, et al. Characterization of the virulence of *Pseudomonas aeruginosa* strains causing ventilator-associated pneumonia. *BMC Infect Dis*. 2020;20(1):909.
51. Carlsson M, Shukla S, Petersson AC, Segelmark M, Hellmark T. *Pseudomonas aeruginosa* in cystic fibrosis: pyocyanin negative strains are associated with BPI-ANCA and progressive lung disease. *J Cyst Fibros*. 2011;10(4):265–71.
52. Tang L, Schramm A, Neu TR, Revsbech NP, Meyer RL. Extracellular DNA in adhesion and biofilm formation of four environmental isolates: a quantitative study. *FEMS Microbiol Ecol*. 2013;86(3):394–403.
53. Chua SL, Ding Y, Liu Y, Cai Z, Zhou J, Swarup S, et al. Reactive oxygen species drive evolution of pro-biofilm variants in pathogens by modulating cyclic-di-GMP levels. *Open Biol*. 2016;6(11):160162.
54. Aguilera-Toro M, Kragh ML, Thomasen AV, Piccini V, Rauh V, Xiao Y, et al. Proteolytic activity and heat resistance of the protease AprX from *Pseudomonas* in relation to genotypic characteristics. *Int J Food Microbiol*. 2023;391–393:110147.
55. Team RC. R: A Language and Environment for Statistical Computing. Vienna, Austria: R Foundation for Statistical Computing; 2021.
56. Henig O, Kaye KS. Bacterial Pneumonia in Older Adults. *Infect Dis Clin North Am*. 2017;31(4):689–713.
57. Gil-Perotin S, Ramirez P, Marti V, Sahuquillo JM, Gonzalez E, Calleja I, et al. Implications of endotracheal tube biofilm in ventilator-associated pneumonia response: a state of concept. *Crit Care*. 2012;16(3):R93.
58. Friedland DR, Rothschild MA, Delgado M, Isenberg H, Holzman I. Bacterial Colonization of Endotracheal Tubes in Intubated Neonates. *Archives of Otolaryngology-Head & Neck Surgery*. 2001;127(5):525–8.
59. Wang J, Liu X, Yu K, Liu M, Qu J, Liu Y, et al. Psl-Dependent Cooperation Contributes to Drug Resistance of *Pseudomonas aeruginosa* in Dual-Species Biofilms with *Acinetobacter baumannii*. *ACS Infect Dis*. 2022;8(1):129–36.
60. Davies G, Wells AU, Doffman S, Watanabe S, Wilson R. The effect of *Pseudomonas aeruginosa* on pulmonary function in patients with bronchiectasis. *Eur Respir J*. 2006;28(5):974–9.
61. Yin G, Huang J, Petela J, Jiang H, Zhang Y, Gong S, et al. Targeting small GTPases: emerging grasps on previously untamable targets, pioneered by KRAS. *Signal Transduct Target Ther*. 2023;8(1):212.
62. Culbertson JE, Toney MD. Expression and characterization of PhzE from *P. aeruginosa* PAO1: aminodeoxyisochorismate synthase involved in pyocyanin and phenazine-1-carboxylate production. *Biochim Biophys Acta*. 2013;1834(1):240–6.
63. Jeffries JL, Jia J, Choi W, Choe S, Miao J, Xu Y, et al. *Pseudomonas aeruginosa* pyocyanin modulates mucin glycosylation with sialyl-Lewis(x) to increase binding to airway epithelial cells. *Mucosal Immunol*. 2016;9(4):1039–50.
64. McCaslin CA, Petrusca DN, Poirier C, Serban KA, Anderson GG, Petrache I. Impact of alginate-producing *Pseudomonas aeruginosa* on alveolar macrophage apoptotic cell clearance. *J Cyst Fibros*. 2015;14(1):70–7.
65. Hill PJ, Scordo JM, Arcos J, Kirkby SE, Wewers MD, Wozniak DJ, et al. Modifications of *Pseudomonas aeruginosa* cell envelope in the cystic fibrosis airway alters interactions with immune cells. *Scientific reports*. 2017;7(1):4761.
66. Janssen KH, Diaz MR, Golden M, Graham JW, Sanders W, Wolfgang MC, et al. Functional analyses of the RsmY and RsmZ small non-coding regulatory RNAs in *Pseudomonas aeruginosa*. *J Bacteriol*. 2018;200(11):e00736-17.

## Publisher's Note

Springer Nature remains neutral with regard to jurisdictional claims in published maps and institutional affiliations.